A Phenomenological Theory of The Pseudogap State

Kai-Yu Yang[1], T. M. Rice[1,2] and Fu-Chun Zhang[1]
[1] *Centre of Theoretical and Computational Physics and Department of Physics, The University of Hong Kong, Hong Kong*
[2] *Institut für Theoretische Physik, ETH Zurich, CH-8093 Zürich, Switzerland*

(Dated: February 4, 2008)

An ansatz is proposed for the coherent part of the single particle Green's function in a doped resonant valence bond (RVB) state by, analogy with the form derived by Konik and coworkers for a doped spin liquid formed by an array of 2-leg Hubbard ladders near half-filling. The parameters of the RVB state are taken from the renormalized mean field theory of Zhang and coworkers for underdoped cuprates. The ansatz shows good agreement with recent angle resolved photoemission (ARPES) on underdoped cuprates and resolves an apparent disagreement with the Luttinger Sum Rule. The transition in the normal state from a doped RVB spin liquid to a standard Landau Fermi liquid, that occurs in the renormalized mean field theory, appears as a quantum critical point characterized by a change in the analytic form of the Green's function. A d-wave superconducting dome surrounding this quantum critical point is introduced phenomenologically. Results are also presented for the Drude weight and tunneling density of states as functions of the hole density.

PACS numbers: 74.20.Mn, 74.25.Jb, 79.60.-i

I. INTRODUCTION

The cuprate superconductors have attracted enormous interest not just because of their high temperature unconventional superconductivity but also because of their highly anomalous properties in the normal phase (for a review see T. Timusk and B. Statt[1]). These show strong deviations from standard Landau Fermi liquid behavior particularly in the underdoped region where the deviations are most evident in the pseudogap (or spin gap) phase. Among the most spectacular of these deviations is the observation of a Fermi surface in photoemission (ARPES) experiments that consists, not of a closed contour, but only of 4 disconnected arcs centered on the Brillouin zone diagonals.[2,3] Pseudogaps in the single particle spectrum truncate the Fermi surface at the saddle points. In addition the density of charge carriers is determined not by the conduction electron density but by the hole density doped into the stoichiometric parent Mott insulator.[1] These facts indicate that the pseudogap phase should be viewed as an anomalous precursor to the stoichiometric Mott insulator.

Very soon after the discovery of the high temperature superconductors and before these anomalous pseudogap properties were measured, Anderson proposed that the key to understanding these unique materials lies in what he called Resonant Valence Bond (RVB) behavior.[4] He proposed a description based on lightly hole doped spin liquid of spin singlets. Rather than forming a fixed array of singlets, strong quantum fluctuations among the antiferromagnetically coupled $S = 1/2$ spins lead to a superposition of singlet configurations, i.e. the bond singlets resonate between many configurations. This elegant concept explains many key features of the pseudogap phase as emphasized in the recent review by Anderson and coworkers.[5] But the strong onsite correlations among the electrons in this precursor to a Mott insulator are difficult to treat analytically. This has hindered the development of complete theory for the RVB phase and the cuprates in general.

In this recent review[5], Anderson and coworkers point out that the early renormalized mean field theory (RMF) introduced by Zhang and coworkers[6] for the RVB phase predicted many of its key features using simple Gutzwiller renormalization factors to describe the strong correlations. In the intervening years much progress has been made on a first principle treatment of these correlations based on gauge theories (for a review see Lee, Nagaosa and Wen[7]). The functional renormalization group (RG) approach developed by Honerkamp and coworkers has also given new insights starting from weak coupling.[8] However, we still lack even a consistent phenomenological description of this anomalous pseudogap phase that ties together key features analogous to the Landau theory for standard Fermi liquids. The purpose of this paper is to take a step in this direction. To this end we introduce an ansatz for the form of the self-energy and thereby for the form of the single particle Green's function. In this we are guided by the recent theory by Konik, Rice and Tsvelik (KRT) for the form of the Green's function in a doped spin liquid consisting of an array of 2-leg Hubbard ladders coupled by long range inter-ladder hopping.[9] By a careful choice of the form of this hopping, KRT could justify a random phase approximation (RPA) to obtain the two dimensional Green's function from the single ladder form. They showed that for a light doping away from one electron/site a novel form of the Green's function, $G(\boldsymbol{k}, \omega)$ resulted. In particular they showed that the behavior of $G(\boldsymbol{k}, 0)$ which enters the Luttinger Sum Rule (LSR)[10], was quite distinct from that of a normal Landau Fermi liquid. The LSR relates the area enclosed by the contours where $G(\boldsymbol{k}, 0)$ changes sign from positive to negative to the total electron density. In a Landau Fermi liquid, sign changes in $G(\boldsymbol{k}, 0)$ occur only through an infinity in $G(\boldsymbol{k}, 0)$ at a closed Fermi surface. In the doped spin liquid, KRT found that the sign changes oc-

cur not only through infinities on Fermi pockets but also through zeroes lying on a separate surface which they call the Luttinger surface of zeroes. The Fermi pockets enclose an area determined by the hole density while the Luttinger surface encloses an area given by the density of one electron per site in the parent stoichiometric ladders. This behavior followed from the form of the self energy in the coherent part of the single ladder Green's function and its modification through the inter-ladder hopping processes. The single ladder Green's function was derived by Essler and Konik only in the weak coupling limit.[11] However, the fact that weak and strong coupling are continuously connected in ladders and that the form is qualitatively similar to that obtained numerically by Troyer et al in strong coupling $t-J$ ladders[12], leads us to believe that this general form is characteristic of doped spin liquid and is not restricted to weak coupling.

In section 2 we introduce our ansatz for the form of the self energy for a two dimensional lightly doped RVB spin liquid. Our ansatz is based on a generalization of the KRT form for the doped spin liquid formed in an array of 2-leg Hubbard ladders.[9] It also contains a Luttinger surface of zeroes which encloses a commensurate density in addition to hole Fermi surface pockets. In this case the Luttinger surface coincides with the so-called umklapp surface introduced by Honerkamp and coworkers[8] as the surface where umklapp scattering processes appear to open up a charge gap in the weak coupling RG flow.

It is also interesting to note that this Green's function is closely related to the form recently proposed by Tai-Kai Ng[13]. He started from the strong coupling limit and introduced spin-charge separation by factorizing single electron operators into a product of spinon and holon operators. Following earlier work by Wen and Lee[14] he introduced a phenomenological attraction between spinon and holon which leads to a binding between spinon and holon. He obtained a form for the Green's function which also contains a coherent quasiparticle pole and has close similarities to our ansatz.

In section 3, we analyze the consequences of our ansatz for a variety of properties. First we obtain the hole density dependence of our psuedogap and other key parameters from the RMF results of Zhang et al.[6] Based on these choices we obtain estimates of the hole density dependence of many observables, e.g. the Fermi velocity v_F and wavevector $\boldsymbol{k}_F$ along the Brillouin zone (nodal) direction, the minimum gap contour near the saddle point (antinodal direction), the tunneling density of state (DOS), the Drude weight, and the shape and form of the hole Fermi pockets. From the phenomenological form of the Green's function we obtain the quasiparticle dispersion and spectral weights that characterize the coherent part of the single electron Green's function. A key point in our phenomenology is that there is a critical hole concentration above which the spin liquid anomalous self-energy vanishes. As consequence there is a form of quantum critical point (QCP) which separates two topologically distinct forms for the Green's function. Below the critical hole density, $G(\boldsymbol{k},0)$ is characterized by coexisting Luttinger surfaces of zeroes and hole pocket Fermi surface of infinities while above the critical concentration $G(\boldsymbol{k},0)$ displays only a closed Fermi surface of infinities as usual in a Landau theory. Many features of this QCP resemble those deduced by Loram and coworkers from an analysis of a variety of experiments[15].

In section 4, we examine how this Green's function is modified when the system enters a d-wave superconducting state. This again is introduced phenomenologically and no attempt is made here to derive the parameters of the superconductivity although we do offer a number of reasons why the hole pockets should have a d-wave superconducting instability.

Lastly section 5 is devoted to further discussions and conclusions.

II. ANSATZ FOR THE SELF ENERGY IN A DOPED RVB SPIN LIQUID

A doped RVB spin liquid has many properties which are quite distinct from the standard Landau Fermi liquid which follows from treating the interactions in perturbation theory. Moreover these anomalous properties cannot be ascribed to a broken symmetry or to the appearance of a new order parameter. As a result it is a challenge to construct a consistent theory even on the phenomenological level of a doped RVB spin liquid. We start with a brief review of the recent work by KRT[9] who could obtain the form of the single particle Green's function $G(\boldsymbol{k},\omega)$ in a doped spin liquid. In particular, they examined the form of the LSR which applies to the zero frequency Green's function $G(\boldsymbol{k},0)$ in the doped spin liquid. The key point about the LSR as emphasized in the famous textbook by Abrikosov, Gorkov and Dzyaloshinskii (AGD)[16] and more recently by Tsvelik[17], is that derivation of the LSR is very general and is not limited to perturbation theory. The LSR relates the total electron density, ρ, to the area in the $\boldsymbol{k}$-space where $G(\boldsymbol{k},0) > 0$. In two dimensions it takes the form

$$\rho = \frac{2}{(2\pi)^2} \int_{G(\boldsymbol{k},0)>0} d^2\boldsymbol{k} \tag{1}$$

An important point that these authors emphasized is that the sign change from positive to negative values of $G(\boldsymbol{k},0)$ is not restricted to an infinity in $G(\boldsymbol{k},0)$ such as occurs at the Fermi surface of a Landau Fermi liquid. It can also occur through a zero in $G(\boldsymbol{k},0)$ as, for example, in the case in the BCS theory of superconductivity. KRT considered a doped spin liquid consisting of an array of two-leg Hubbard ladders. At half-filling in a single ladder the Fermi surface consists of four points without interactions, but it is completely truncated when the repulsive interactions which lead to both spin and charge gaps, are introduced. All spin and charge correlation functions

are strictly short range so that this system is a true spin liquid.

An explicit form for the single particle Green's function has been derived by Konik and coworkers in the limit of weak repulsion.[11,18] Around each of the four Fermi points $G(k,\omega)$ can be split into coherent and incoherent parts,

$$G_a^L(k,\omega) = \frac{z_a(\omega+\epsilon_a(k))}{\omega^2-\epsilon_a^2(k)-\Delta^2} + G_{inc} \tag{2}$$

Here $\epsilon_a(k)$ is the bare dispersion near the corresponding Fermi wavevector k_{Fa}, z_a is quasiparticle weight ~ 1, and Δ the single particle gap. Note while the coherent part has a form similar to the diagonal Green's function in BCS theory, there is no off-diagonal component of the Green's function in this case. This general form is also compatible with the numerical results of Troyer et al for the strong coupling limit[12]. $G_a^L(k,0)$ changes sign from positive to negative through a zero in $G_a^L(k,0)$ which occurs when $\epsilon_a(k)$ passes through zero as k crosses k_{Fa}, and the area with $G_a^L(k,0)>0$ is unchanged by the interactions, satisfying the LSR.

Starting from this result, KRT could derive $G_a^L(\boldsymbol{k},\omega)$ for an array of 2-leg Hubbard ladders coupled by a particular form of long range inter-ladder hopping chosen so that it could be treated using a random phase approximation (RPA)

$$G_a^{RPA}(\boldsymbol{k},\omega) = 1/\{G_a^L(k,\omega)^{-1} - t_\perp(k_\perp)\} \tag{3}$$

where $\boldsymbol{k} = (k,k_\perp)$. They showed that this form, for values of $t_\perp$ large enough, leads to the appearance of electron and hole pockets distinct from the lines of zeroes in $G_a^{RPA}(\boldsymbol{k},0)$. The zero contours remain as lines at $k=k_{Fa}$, independent of the transverse component of the wavevector, $k_\perp$. In the presence of hole doping, the hole pocket expands and the electron pocket shrinks. In this doped spin liquid $G_a^{RPA}(\boldsymbol{k},0)$ has sign changes both through infinities along the Fermi pockets and through zeroes located on the lines $k=k_{Fa}$. Note although the zeroes lines appear at incommensurate wavevectors in general and not at the Brillouin zone as in a standard Bloch insulator, the total area they enclose is commensurate and equals 1 electron /site, irrespective of the inter-ladder hopping strength. The final form obtained by KRT for the coherent part is

$$G_a^{RPA}(\boldsymbol{k},\omega) = \frac{z_a}{\omega-\epsilon_a(k)-t_\perp(k_\perp)-\Delta^2/(\omega+\epsilon_a(k))} \tag{4}$$

This can be interpreted as a ladder self energy $\Sigma_L(k,\omega) = \Delta^2/(\omega+\epsilon_a(k))$, where $\epsilon_a(k)=0$ at the k-points where the gap opens up in the parent insulating two-leg Hubbard ladder array.

In this work we consider doping a two-dimensional resonant valence bond insulator. We start from the RMF for such an insulator. This approximation treats the effect of strong correlations through renormalization factors calculated by a description that goes back to early work by Gutzwiller[19]. The renormalized $t-J$ Hamiltonian takes the form of an effective Hamiltonian[6]

$$H_{eff} = g_t T + g_s J \sum_{\langle i,j\rangle} \boldsymbol{S}_i \cdot \boldsymbol{S}_j \tag{5}$$

with the kinetic, T, and spin energy terms modified by factors g_t and g_s respectively

$$\begin{aligned} g_t &= \frac{2x}{1+x}, \\ g_s &= \frac{4}{(1+x)^2} \end{aligned} \tag{6}$$

for a hole doping of x per site. At half-filling $g_t=0$ leaving only the magnetic energy. The RVB ansatz factorizes the spin energy introducing both Fock exchange, $\chi_{i,j} = \left\langle c^\dagger_{i,\sigma} c_{j,\sigma}\right\rangle$ and pairing, $\Delta_{i,j} = \langle c_{i,\sigma} c_{j,\sigma}\rangle$ expectation values. The factorization procedure is not unique but the spin quasiparticle dispersion that results is unique, $E_{\boldsymbol{k}} = (3g_sJ/8)(\cos^2 k_x + \cos^2 k_y)^{1/2}$. Upon hole doping $g_t>0$, and coherent quasiparticle poles with a small weight g_t appear in the single particle Green's function. By analogy with the KRT form for the doped spin liquid discussed above, we make the following ansatz for the coherent part of $G(\boldsymbol{k},\omega)$ in a doped RVB spin liquid

$$G^{RVB}(\boldsymbol{k},\omega) = \frac{g_t}{\omega-\xi(\boldsymbol{k})-\Delta_R^2/(\omega+\xi_0(\boldsymbol{k}))} + G_{inc} \tag{7}$$

where $\boldsymbol{k}=(k_x,k_y)$,

$$\begin{aligned} \xi_0(\boldsymbol{k}) &= -2t(x)(\cos k_x + \cos k_y) \\ \Delta_R(\boldsymbol{k}) &= \Delta_0(x)(\cos k_x - \cos k_y) \\ \xi(\boldsymbol{k}) &= \xi_0(\boldsymbol{k}) - 4t'(x)\cos k_x \cos k_y \\ &\quad -2t''(x)(\cos 2k_x + \cos 2k_y) - \mu_p \end{aligned} \tag{8}$$

Eq.7 is analogy to Eq.4 for the coupled ladder system, and $\xi(\boldsymbol{k})-\xi_0(\boldsymbol{k})$ is analogy to $t_\perp(k_\perp)$ in Eq.4. In the renormalized dispersion we include hopping terms out to 3rd nearest neighbor with coefficients

$$\begin{aligned} t(x) &= g_t(x)t_0 + \frac{3}{8}g_s(x)J\chi, \\ t'(x) &= g_t(x)t'_0, \\ t''(x) &= g_t(x)t''_0 \end{aligned} \tag{9}$$

The RVB gap magnitude function $\Delta_0(x)$ is also taken from the RMF theory[6]. The parameter μ_p represents a shift of the energy band so that the chemical potential is always the zero of the energy. We determine μ_p from the LSR on the total electron density.

First we consider the limit of zero doping, $x\to 0$. In this case $g_t(x)\to 0$ and the quasiparticle dispersion reduces to the spinon dispersion and the quasiparticles have the vanishing weight in this limit in the single particle Green's function, $G(\boldsymbol{k},\omega)$. At small but finite x the zero frequency Green's function $G^{RVB}(\boldsymbol{k},0)$ that enters the LSR has lines of zeroes when $\xi_0(\boldsymbol{k})(=$

$-2t(x)(\cos k_x + \cos k_y)) = 0$. The Luttinger contour of zeroes in $G^{RVB}(\boldsymbol{k}, 0)$ then consists of straight lines connecting the points $(\pm\pi, 0)$ and $(0, \pm\pi)$. This Luttinger contour coincides with the antiferromagnetic (AF) Brillouin zone. But more relevantly it coincides with the umklapp surface which appears in functional RG calculations on the weak coupling 2D $t - t' - U$ Hubbard model. Honerkamp[8], Laeuchli and coworkers[20] found that umklapp scattering processes in both particle-hole and particle-particle channel which connect points on this surface grew strongly at low energies and temperatures leading them to propose that an energy gap would open up on this surface below a critical scale. Further because of a close analogy to the behavior found in the case of a half-filled 2-leg Hubbard ladder, they proposed that this gap was not driven by long range order, but rather was a sign that a RVB spin liquid with short range order would form below a critical scale. Thus our ansatz for the Green's function is fully consistent with these proposals.

A second feature that follows from our ansatz for $G^{RVB}(\boldsymbol{k}, \omega)$ is the appearance of hole pockets at finite hole doping. These will be reviewed in detail in the next section. The hole pockets define Fermi surfaces where $G^{RVB}(\boldsymbol{k}, 0)$ changes sign through infinities and contain a total area equal the hole density. The LSR is satisfied since the area with $G^{RVB}(\boldsymbol{k}, 0) > 0$ is bounded by the Luttinger surface which contains 1 el/site, minus four hole pockets which have a total area related to the hole density.

The phenomenological form $G^{RVB}(\boldsymbol{k}, 0)$ for a hole doped RVB spin liquid can be straightforwardly generalized to a d-wave superconducting state

$$\begin{aligned} & G^S_{coh}(\boldsymbol{k}, \omega) \\ = \; & g_t / [\omega - \xi(\boldsymbol{k}) - \Sigma_R(\boldsymbol{k}, \omega) \\ & - |\Delta_S(\boldsymbol{k})|^2 / (\omega + \xi(\boldsymbol{k}) + \Sigma_R(\boldsymbol{k}, -\omega))] \end{aligned} \quad (10)$$

where $\Sigma_R(\boldsymbol{k}, \omega)$ is the RVB spin liquid self energy from Eq.[7]

$$\Sigma_R(\boldsymbol{k}, \omega) = |\Delta_R(\boldsymbol{k})|^2 / (\omega + \xi_0(\boldsymbol{k})) \quad (11)$$

and $\Delta_S(\boldsymbol{k})$ is the d-wave superconducting gap function. To analyze the LSR on $G^S_{coh}(\boldsymbol{k}, 0)$ we note first that $\Sigma_R(\boldsymbol{k}, 0) \to \infty$ on the surface where $\xi_0(\boldsymbol{k}) = 0$. Thus $G^S_{coh}(\boldsymbol{k}, 0)$ continues to have a Luttinger surface of zeroes on the umklapp surface as in the normal RVB spin liquid. However, there is now an additional set of Luttinger surfaces defined by the contour that satisfy

$$\xi(\boldsymbol{k}) + \Sigma_R(\boldsymbol{k}, 0) = 0$$

But these are just the Fermi surface of the four hole pockets in the normal phase which have now been converted to a Luttinger surface of zeroes in the superconducting state. Thus the form Eq.[10] continues to satisfy the LSR.

Lastly we remark that along the Brillouin zone diagonals both $\Delta_R(\boldsymbol{k})$ and $\Delta_S(\boldsymbol{k})$ vanish in our phenomenological form. As a result exactly along these directions there is only a single quasiparticle pole which crosses the Fermi energy at a Fermi wavevector determined by $\xi(\boldsymbol{k})|_{\boldsymbol{k}=(k_F, k_F)} = 0$.

Our phenomenological form for G^{RVB} in the normal and superconducting phases are similar but not identical to several other recent proposals. It is very close to the form Tai-Kai Ng[13] derived based on spin-charge separation but with an added phenomenological attraction between spinon and holon which leads to binding and therefore to quasiparticle poles and a self energy form similar to Eq.[11]. He, however, restricted his analysis to the case of only nearest neighbor hopping. Earlier Norman and coworkers from an analysis of ARPES data on BSCCO samples around optimal doping introduced a d-wave superconducting self energy modified to included both normal state single particle scattering and pair scattering.[21] Recently Honerkamp[22] has speculated on an adaptation of the form introduced by Norman et al to describe a truncation of the Fermi surface through the opening of energy gap in the antinodal regions near $(\pm\pi, 0)$, $(0, \pm\pi)$ as a phenomenological description of the RVB spin liquid.

III. ELECTRONIC PROPERTIES OF THE NORMAL PSEUDOGAP PHASE

In this section we discuss the electronic properties that follow from our phenomenological form for the Green's function and compare these to experiments on the normal pseudogap state.

We begin with the LSR shown in Eq.[1]. In Fig.1(a-e) we show that the contours on which $G^{RVB}(\boldsymbol{k}, \omega = 0)$, defined in Eq.[7], changes sign. We chose values for hopping parameters in Eq.[9], appropriate to $Ca_{2-x}Na_xCuO_2Cl_2$. The underlying band structure parameters were obtained by a tight-binding fit to the antibonding $3d_{x^2-y^2} - 2p_{x(y)}$ band calculated by Mattheiss[23]. These were then renormalized by the Gutzwiller factors defined in Eq.[6], leading to the values shown in Fig.2. The sign changes in $G^{RVB}(\boldsymbol{k}, \omega = 0)$ occur on a Luttinger surface of zeroes, which coincides with the umklapp surface, and on a Fermi pocket of infinities. The parameter μ_p was adjusted at each x to give the correct area for the hole pockets (see Fig.2).

As we can see from Fig.1, the hole pocket evolves gradually into a more normal surface in panel(e) as x increase. The spectral weight of the quasiparticle pole varies strongly around the pocket as illustrated in Fig.3. In particular it is very small on the outer edge of the pocket closest to the Luttinger surface of zeroes and vanishes completely along the nodal directions ((1,1) directions). Along this direction there is only a single sign change in $G^{RVB}(\boldsymbol{k}, \omega = 0)$ at the inner pocket edge.

In Fig.4, the dispersion of the quasiparticle poles $E_i(\boldsymbol{k})$ in the coherent part of G^{RVB} together with their spectral weight, $z_i(\boldsymbol{k})$, are shown. We see that in general there are two quasiparticle bands $E_i(\boldsymbol{k})$ with strongly

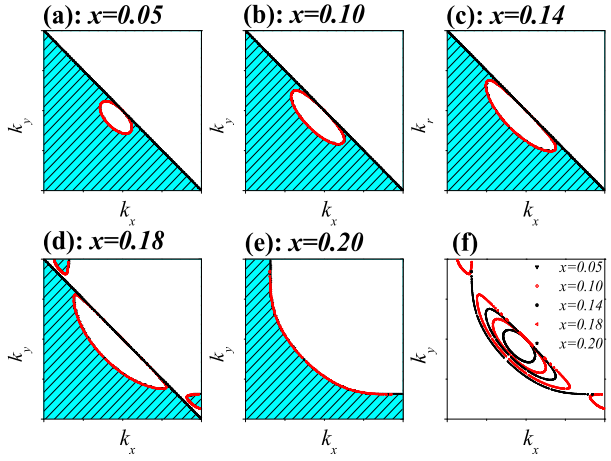

FIG. 1: (Color online) Contours on which $G(\boldsymbol{k},0)$ changes sign at various hole concentrations x are shown in (a)-(e). In the shaded area $G(\boldsymbol{k},0) > 0$, satisfying the Luttinger Sum Rule. In the normal pseudogap phase, the line connecting $(\pi,0)-(0,\pi)$ is the Luttinger surface of zeroes and the pockets in the thick line represent the infinities of $G(\boldsymbol{k},0)$. The values of the parameters used here are given in Fig.2. The evolution of the contours of infinities in $G(\boldsymbol{k},0)$ is illustrated in (f).

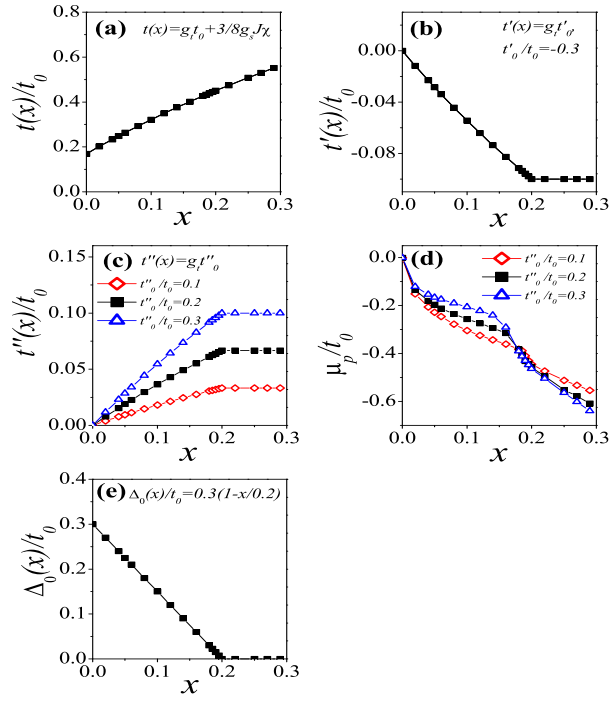

FIG. 2: (Color online) The values of the parameters $t(x)$, $t'(x)$, $t''(x)$, μ_p and $\Delta(x)$ that enter in Eq.[8,9] used in the present calculations. ($\chi = 0.338$, $J/t_0 = 1/3$) Results presented in the text are for a choice of $t'_0/t_0 = -0.3$, $t''_0/t_0 = 0.2$, estimated from the calculated band structure of $Ca_2CuO_2Cl_2$.[23]

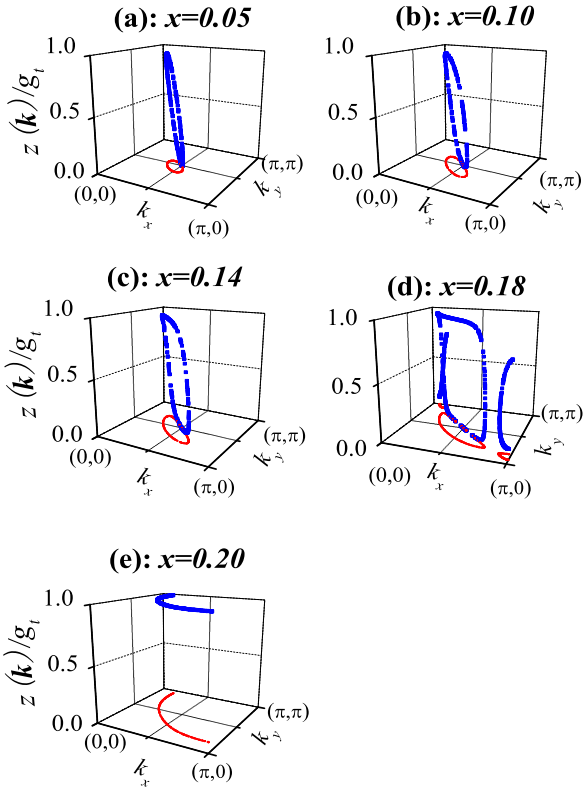

FIG. 3: (Color online) The spectral weight distribution $z(\boldsymbol{k})/g_t$ around the hole quasiparticle pockets in the normal pseudogap phase.

varying spectral weight. Over most of the Brillouin zone the bands are separated by an energy gap with only the lower band occupied. The distribution of spectral weight between the two bands is determined by the proximity to the umklapp surface. Near this surface the weight is equally divided but away from this surface only a small admixture is induced by the anomalous self energy Σ_R. Also along the nodal directions $\Sigma_R \to 0$, so that in these directions the two bands coalesce into a single band.

In order to compare to ARPES experiments on $Ca_{2-x}Na_xCuO_2Cl_2$[3], we prepared a single plot which combines contours of the hole Fermi pockets and also the minimum energy gap lines in other parts of zone. These are illustrated in Fig.5 together with the ARPES results. There is good agreement between the two sets of curves with the exception of the outer edge of the hole pockets which has not been reported in the ARPES experiments. The predicted spectral weight of the quasiparticle band on these outer edges is very small (see Fig.3). Nonetheless it would be important to search more closely for a weak signal on this edge. In Fig.6, we plot the dispersion of the lower quasiparticle band $E(\boldsymbol{k})$ on the "Fermi surface" and on the hole pockets for several dopings. The

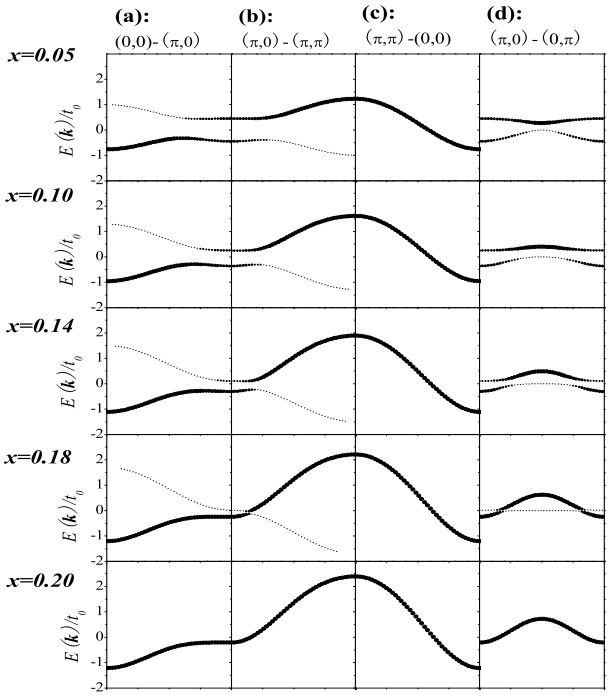

FIG. 4: (Color online) Quasiparticle dispersion in the normal pseudogap phase (Eq.[7]) along some high symmetry directions. The thickness of the lines is proportional to the spectral weight $z(\boldsymbol{k})/g_t$ of the quasiparticle.

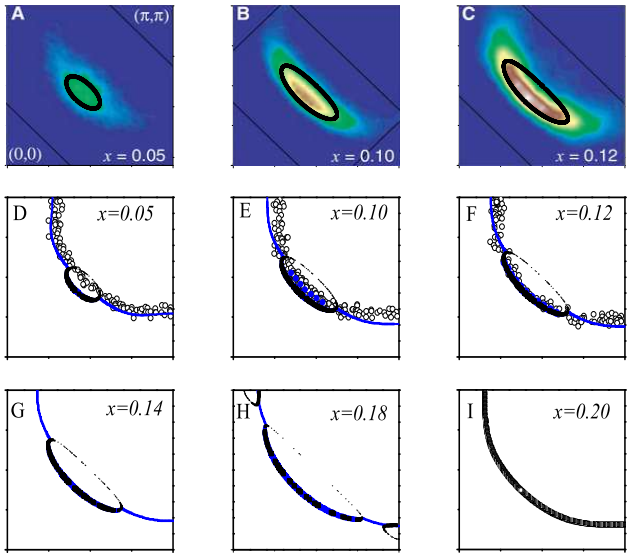

FIG. 5: (Color online) Comparison between our theory and some recent ARPES experiments on $Ca_{2-x}NaCuO_2Cl$ by K. M. Shen et al.[3] The experimental results are re-plotted in panels (A-F). Panels (A-C) show the distribution of spectral weight in the Brillouin zone within a $\pm 10meV$ window around the Fermi level. The open/solid circles in panels (D-F) are detected by this experiment to determine the Fermi surface. The pockets in panel (A-I) show the infinities of $G(\boldsymbol{k}, 0)$ in the normal pseudogap phase. The "Fermi surfaces" (blue and black curves) shown in panels (D-I) are defined by the minimum distance from the lower quasiparticle band to the Fermi level in our calculation along radial directions centered at (π, π). The thickness of the curve in panels (D-I) represents the spectral weight $z(\boldsymbol{k})/g_t$ of the quasiparticle.

angular dependence of $|E(\boldsymbol{k})|$ on the "Fermi surface" is shown in panel (e). The dispersion drops to zero rather sharply as the angle touches the pocket direction.

In Fig.7 we show the hole density dependence of the two features, the Fermi wavevector, k_F (with $\boldsymbol{k}_F = k_F(1,1)$) at the hole pocket along the nodal line $(1,1)$ and the intercept of the minimum energy gap line at the Brillouin zone boundary connecting $(\pi,0)-(\pi,\pi)$ antinodal-k_F^A (with $\boldsymbol{k}_F^A = (k_F^A, \pi)$). Again the agreement is very good with ARPES experiments on $Ca_{2-x}Na_xCuO_2Cl_2$[3]. These two wavevectors have been interpreted as key parameters of an underlying Fermi surface. But such an interpretation clearly violates the LSR since the enclosed area would require electron doping in contrast to our ansatz for the Green's function. As we remarked earlier, our ansatz reconciles the ARPES measurements and the LSR.

Also in Fig.7 we show the Fermi velocity v_F along the nodal direction. This shows rather more variation with the hole doping, x, than the direct calculations from the Gutzwiller projected variational wavefunction[24] but the qualitative behavior is similar. However, it deviates substantially from experiment with increasing x. The discrepancy of v_F at large x could be due to the oversimplified model.

Another quantity of interest is the coherent quasiparticle contribution to the tunneling density of state (DOS) defined as

$$N_T(\omega) = \sum_{\boldsymbol{k}, i=1,2} z_i(\boldsymbol{k}) \delta(\omega - E_i(\boldsymbol{k})) \tag{12}$$

The value at the chemical potential, $N_T(0)$ is shown for a series of hole densities in Fig.8(a). $N_T(0)$ rises linearly as the hole density x is increased from zero in the pseudogap phase. This behavior is similar to the Drude weight, $D_{\mu\upsilon}$, calculated by integrating around the Fermi surfaces of the hole pockets

$$D_{\mu\upsilon} = \frac{2}{(2\pi)^2} \frac{e^2}{\hbar} \int \frac{v_\mu v_\upsilon}{|\boldsymbol{v}|} dS_F \tag{13}$$

In the square lattice $D_{\mu\upsilon}$ is a diagonal tensor with element $D_{\mu\mu}$ shown in Fig.8(b).

The density dependence of the RVB gap parameter, $\Delta_0(x)$ was taken from the RMF results of Zhang et al.[6] This gives a linear drop in Δ_0 with $\Delta_0(x) \to 0$, as $x \to x_c$ (see in Fig.2(e)). We have chosen a value of $x_c = 0.2$. This linear drop in $\Delta_0(x)$ as x increases is in line

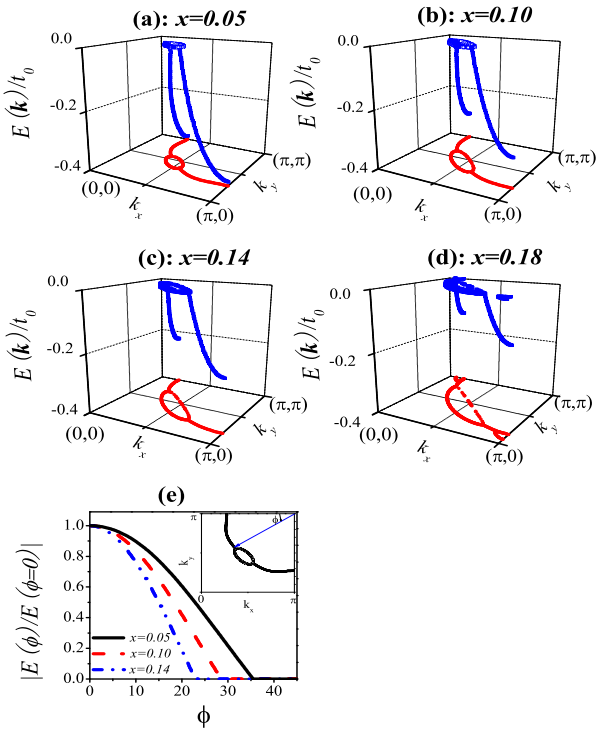

FIG. 6: (Color online) Panel(a-d) show the dispersion of the lower quasiparticle band $E(\boldsymbol{k})$ on the "Fermi surface" and on the hole pockets for various dopings. In panel(e) we show the angular dependence of $|E(\boldsymbol{k})|$ on the "Fermi surface". ϕ is defined in the inset of panel (e).

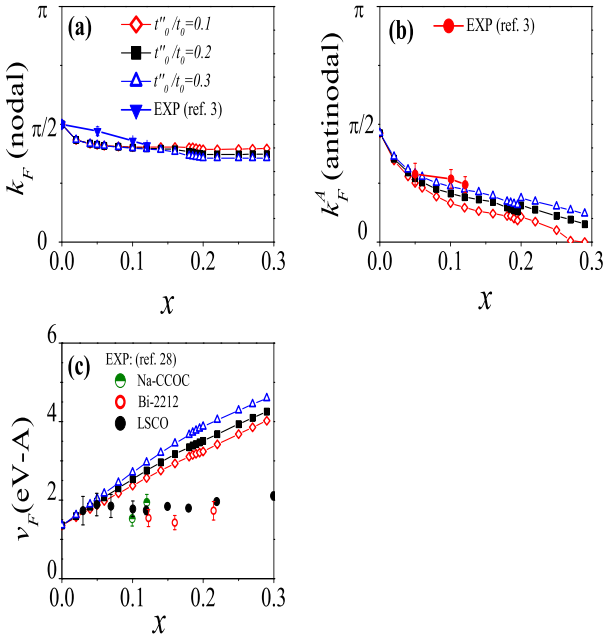

FIG. 7: (Color online) Nodal Fermi wavevector k_F, 'antinodal Fermi wavevector' k_F^A, Fermi velocity v_F (with values $t_0 = 0.5eV$, lattice constant $a = 4.0\mathring{A}$). The experimental data in panel (a,b) for nodal and 'antinodal Fermi wavevector' are for $Ca_{2-x}Na_xCuO_2Cl_2$[3] while the experimental results in panel (c) are for $Ca_{2-x}Na_xCuO_2Cl_2$, $La_{2-x}Sr_xCuO_4$, and $Bi_2Sr_2CaCu_2O_{8+\delta}$[28].

with ARPES experiments as emphasized in the recent review by Anderson et al.[5] The vanishing of $\Delta_0(x)$ at $x = x_c$ causes a change in the form of $G(\boldsymbol{k}, \omega)$ with a transition from the doped spin liquid RVB character to that of a standard Landau Fermi liquid. Then contours of sign changes in $G(\boldsymbol{k}, 0)$ that enter the LSR change their topology and the Luttinger surface of zeroes disappears. Only a standard closed Fermi surface of infinities exists at $x > x_c$.

The detailed form of the transition from a doped RVB spin liquid to a Landau Fermi liquid depends on the band parameters. For the choice that we made to correspond to $Ca_{2-x}Na_xCuO_2Cl_2$, there is an additional topological change in the LSR contours as $x \to x_c$. As illustrated in Fig.1, for a narrow range of $x \lesssim x_c$ a new set of electron Fermi pockets appear close to the saddle points, outside the Luttinger surface of zeroes. These new electron pockets merge with the hole pockets inside the Luttinger surface of zeroes at $x = x_c$ to give a Fermi surface that crosses the umklapp surface at $x > x_c$. In our parameter choice the saddle points in the band structure are occupied for a range of hole densities for $x \gtrsim x_c$ which requires that the Fermi surface cross the umklapp surface in this

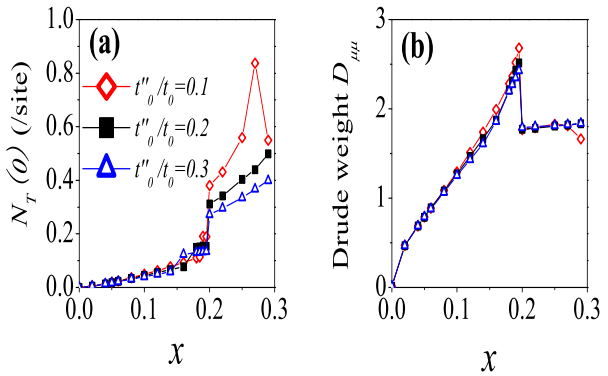

FIG. 8: (Color online) Density of states at the Fermi level $N_T(0)$ and the Drude weight $D_{\mu\mu}$ in the normal pseudogap phase.

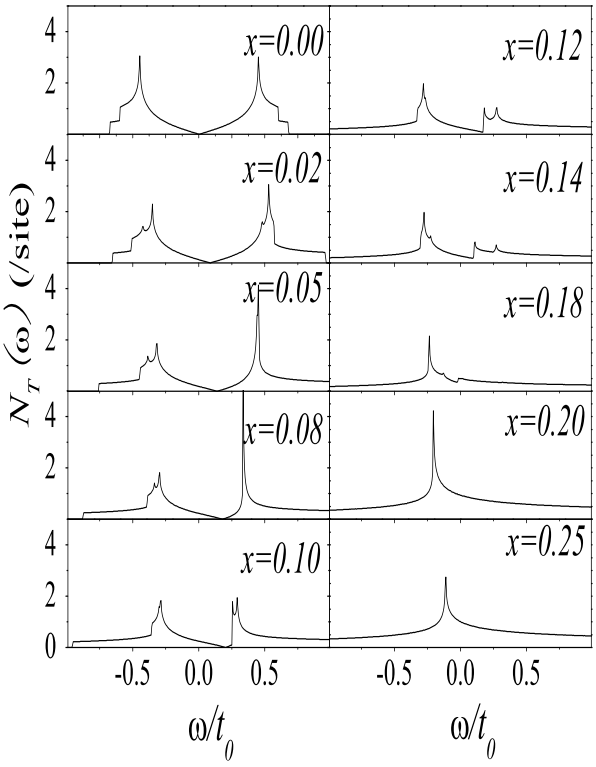

FIG. 9: (Color online) Density of states $N_T(\omega)$ in the normal pseudogap phase. The zero energy values $N_T(0)$ are shown in Fig.8(a).

density range. For this parameter choice, there are two closely spaced topological changes in the LSR contours. The first is a Lifschitz-type transition in which the shape of the Fermi surface of infinities undergoes a topological change. The second at $x = x_c$ is a quantum critical point (QCP) associated with opening of a single particle gap at the onset of the RVB spin liquid for $x < x_c$ leading to a Luttinger surface of zeroes coinciding with the umklapp surface.

These two transitions cause singularities in the density dependence of the DOS and the Drude weight as illustrated in Fig.8. The strongest singularity appears at the QCP at $x = x_c$. A substantial jump appears in the DOS at $x = x_c$. The DOS continues to rise as x increases beyond x_c which is associated with the approach of the Fermi energy to the van Hove singularity at the saddle points in the band structure. A divergence of the DOS at the Fermi energy at $x > x_c$ has not been observed to our knowledge but this might be due to different band parameters or possibly to a suppression of the divergence due to impurity scattering. The full energy dependence of the DOS is shown in Fig.9.

The QCP in our phenomenological theory is qualitatively similar to that inferred by Loram, Tallon and collaborator from experiments[15,25]. Their analysis emphasized the singularities in thermodynamic quantities such as specific heat, magnetic susceptibility etc. Our phenomenological theory is restricted at present to zero temperature and so is not suitable for detailed comparison. However, we note that the main conclusion they drew, that a partial gap opened up at $x < x_c$, is in agreement with our phenomenological theory.

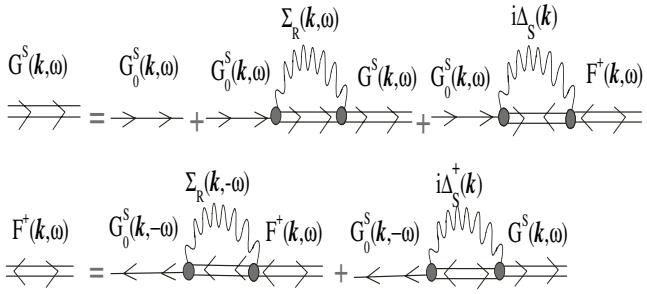

FIG. 10: (Color online) Regular and anomalous Green's functions $G(\boldsymbol{k},\omega)$, $F^\dagger(\boldsymbol{k},\omega)$ which appear in the coupled Eq.[14,15].

IV. ELECTRONIC PROPERTIES OF THE SUPERCONDUCTING STATE

We turn now to the evolution of the electronic properties when the system enters a d-wave superconducting state. Superconductivity is introduced by the addition of the new term in the self-energy which follows from the standard Green's function theory of a superconductor[16]. Solving the coupled equations which connect the regular ($G^S(\boldsymbol{k},\omega)$) and anomalous ($F(\boldsymbol{k},\omega)$) Green's functions (see Fig.10)

$$(\omega - \xi(\boldsymbol{k}) - \Sigma_R(\boldsymbol{k},\omega))G^S(\boldsymbol{k},\omega) \\ -i\Delta_S(\boldsymbol{k})F^\dagger(\boldsymbol{k},\omega) = 1 \quad (14)$$

$$(-\omega - \xi(\boldsymbol{k}) - \Sigma_R(\boldsymbol{k},-\omega))F^\dagger(\boldsymbol{k},\omega) \\ -i\Delta_S^\dagger(\boldsymbol{k})G^S(\boldsymbol{k},\omega) = 0 \quad (15)$$

leads the result quoted earlier in Eq.[10]

$$[\omega - \xi(\boldsymbol{k}) - \Sigma_R(\boldsymbol{k},\omega) \\ -\frac{|\Delta_S(\boldsymbol{k})|^2}{(\omega + \xi(\boldsymbol{k}) + \Sigma_R(\boldsymbol{k},-\omega))}]G^S(\boldsymbol{k},\omega) = 1 \quad (16)$$

The gap function is assumed to have a d-wave form and it is related to the anomalous Green's function

$$\Delta_S(\boldsymbol{k}) = \int d^2\boldsymbol{k}' d\omega g(\boldsymbol{k}-\boldsymbol{k}')F(\boldsymbol{k}',\omega) \quad (17)$$

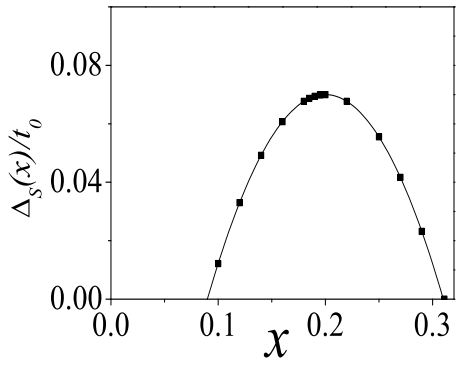

FIG. 11: (Color online) The phenomenological form of the superconducting gap that follows from a parabolic relation for $T_c(x)$: $\Delta_S(x)/t_0 = 0.07(1 - 82.6(x - 0.2)^2)$.

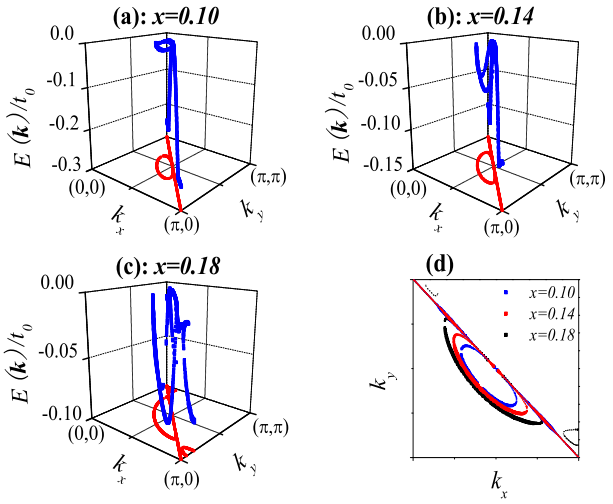

FIG. 12: (Color online) The dispersion (panels (a-c)) and weight (panel (d)) on the Luttinger surface with nonzero superconducting gap. There are 2 bands below the Fermi level, and shown here is the one closer to Fermi level. Around $(\pi, 0)$ and $(0, \pi)$, there is a substantial part of the spectral weight located at the lower band, only a small part remains on the band closer to the Fermi level as indicated in Fig13.

where $g(\boldsymbol{k} - \boldsymbol{k}')$ is the d-wave pairing interaction.

The strength of the superconductivity is determined by the magnitude of the gap squared. We assume a simple parabolic form for $T_c(x)$[26] to mimic experiment (see Fig.11) and the gap is scaled with the superconducting, T_c.

We begin by examining the form of the LSR in the superconducting state. By inspecting the function $G^S_{coh}(\boldsymbol{k}, 0)$ defined in Eq.[10] we see at once that the denominator diverges on the contours defined by $\xi_0(\boldsymbol{k}) = 0$ and by $\xi(\boldsymbol{k}) + \Sigma_R(\boldsymbol{k}, 0) = 0$. These are the same LSR contours that occur in the normal state. The only difference is that the second set of contours now define zeroes of $G^S_{coh}(\boldsymbol{k}, 0)$ not infinities. The Fermi surface of the hole pockets is gapped except along the nodal line where both $\Delta_R(\boldsymbol{k}) = \Delta_S(\boldsymbol{k}) = 0$. The form (10) for $G^S_{coh}(\boldsymbol{k}, \omega)$ then continues to satisfy the LSR.

In the superconducting state the quasiparticle poles are given by solutions to a quartic equation

$$(\omega^2 - \xi^2(\boldsymbol{k}))(-\omega^2 + \xi_0^2(\boldsymbol{k})) + 2\Delta_R^2(\boldsymbol{k})(\omega^2 - \xi_0(\boldsymbol{k})\xi(\boldsymbol{k})) + \Delta_S^2(\boldsymbol{k})(\omega^2 - \xi_0^2(\boldsymbol{k})) - \Delta_R^4(\boldsymbol{k}) = 0 \quad (18)$$

which results in a further splitting of the quasiparticle bands. These are illustrated in Fig.13 for a number of hole densities. The spectral weight redistribution is small when the original quasiparticle energies are away from the chemical potential. This can be seen for example in panel (d) of Fig.13 which shows the quasiparticle bands and their weight along the umklapp surface connecting $(\pi, 0) - (0, \pi)$. Here we see comparable weights only when the hole Fermi pockets are nearby.

The superconducting energy gap modifies the DOS, $N_T(\omega)$. As illustrated in Fig.14 the opening of the superconducting gap along the Fermi pockets (shown in Fig.12) leads to a pseudogap in $N_T(\omega)$ accompanied by van Hove singularities at the gap maxima. Note these van Hove singularities do not occur at the usual antinodal $\boldsymbol{k}$-points $(\pm\pi, 0)$, $(0, \pm\pi)$ but rather on the extremities of the hole Fermi pockets. This is because the form Eq.[10] we chose for the superconducting state does not represent a merging of the two gaps $\Delta_R(\boldsymbol{k})$ and $\Delta_S(\boldsymbol{k})$, rather both gaps keep their own identity. Further consideration of this point would require a better microscopic understanding of the coexistence of d-wave superconductivity with the RVB spin liquid correlations than our simple phenomenological ansatz.

Another clear feature in $N_T(\omega)$ is the van Hove singularity associated with antinodal saddle points in the RVB quasiparticle bands at negative energy. This feature does not appear in the STM experiments. This could be due to the strong local variations in the hole density.

V. DISCUSSION AND CONCLUSION

The ansatz for the Green's function Eq.[7] is motivated in the first place by the form of the Green's function derived recently by Konik and coworkers[9,18] for a doped spin liquid composed of an array of 2-leg Hubbard ladders. A second important input is the renormalized mean field derived many years ago by Zhang and coworkers[6]. As emphasized recently by Andseron and coworkers[5], the RMF, although it treats the strong correlations simply by Gutzwiller renormalization factors, agrees qualitatively and even at times quantitatively with the results of variational Monte Carlo (VMC) calculations using Gutzwiller

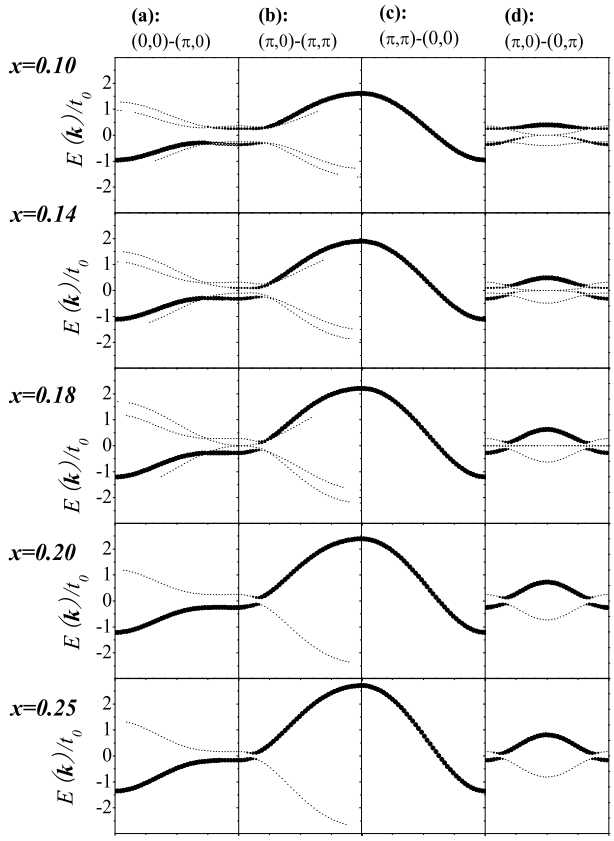

FIG. 13: (Color online) Quasiparticle dispersion $E(\boldsymbol{k})$ in the superconducting state (Eq.[10]) along high symmetry directions. The thickness of the lines is proportional to the spectral weight $z(\boldsymbol{k})/g_t$.

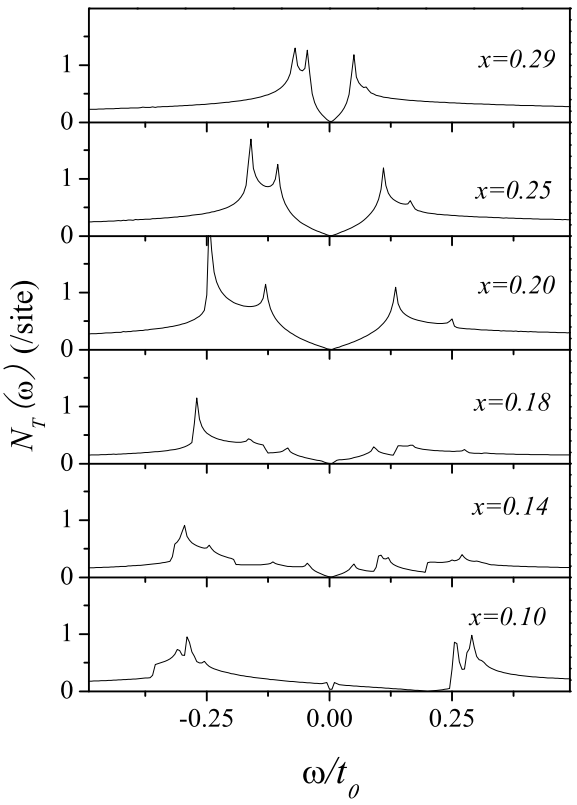

FIG. 14: (Color online) Density of states $N_T(\omega)$ in the presence of a nonzero superconducting gap. The additional peaks closest to Fermi level are determined by the superconducting gap which opens on the hole pockets for $x < x_c$. For $x \geq x_c$ the peaks come from the antinodal directions for $(\pm\pi, 0)$, $(0, \pm\pi)$.

projected wavefunctions[24]. The RMF and VMC calculations at finite doping rely on a broken symmetry to introduce a gap at the Fermi energy. However, in the underdoped region the gap at the antinodal regions ($\sim J$) is much larger than the expected superconducting transition temperature T_c as estimated for example by Wen and Lee[14]. So one should expect this gap to persist in the normal state at temperatures $T \geq T_c$, and so should be a property of the RVB spin liquid and not related to a broken symmetry. Another key feature of the underdoped region is that the Drude weight scales as the hole concentration. As a result the simplest explanation for these two properties is that the Fermi surface is partially truncated in a doped RVB spin liquid rather like the partial truncation that occurs through spin density waves in Cr and its alloys before the commensurate antiferromagnetic state is reached[27]. Here the key difference to the Cr alloys is the absence of a broken symmetry and long range order. Theses properties are reconciled by our ansatz for the normal state. In the superconducting state we introduced Δ_S and Δ_R as separate gaps whereas in the RMF and VMC calculations there is only a single gap function opening up along a single Fermi surface. So it would appear that our ansatz is qualitatively different to the RMF and VMC theories in the superconducing state. However, one cannot be sure of this since the key quantity is the zero frequency Green's function $G(\boldsymbol{k}, 0)$ which is not directly available from a variational wavefunction. We note that there have been recent reports on the numerical study of the pseudogap phase by using cluster perturbation theory (CPT)[29] and by the dynamical mean field theory (DMFT)[30] of the 2-Dimension Hubbard model.

Our ansatz does not deal with the origin of the d-wave superconductivity *per se*. The relevant issue is the stability of the normal state as a doped RVB state. This issue was addressed in the case of the doped array of 2-leg Hubbard ladders by KRT[9]. They showed that strong residual interactions acting on the hole pockets lead to a d-wave superconducting state or possibly a spin density wave state depending on the parameters. There is strong reason to believe that similar effects should occur here in

the 2-dimensional doped RVB spin liquid. Indeed such effect were conjectured by Honerkamp[8], Laeuchli and coworkers[20] in their analysis of the functional RG calculation for the 2-dimensional $t-t'-U$ Hubbard model. On a qualitative level we know that the RVB spin liquid has enhanced response in both d-wave pairing and antiferromagnetic channels so that the Fermi pockets are moving in a background which is highly polarizable in both these channels which can lead to corresponding instabilities. The challenge is to develop a proper microscopic theory to describe the competition between the two instabilities. Note unlike the case of heavy fermions where a superconducting dome straddles the QCP associated with onset of long range AF order[31], here superconductivity seems to be most stable near the onset of the RVB phase with short range correlations. The good agreement that this ansatz displays with many properties of the anomalous normal state in the pseudogap region is evidence that it contains at least elements of the correct physics.

The authors acknowledge the support from Centre of Theoretical and Computational Physics and Visiting Professorship at The University of Hong Kong. T. M. Rice also acknowledges support at ETH from the MANEP program of the Swiss National Foundation.

[1] T. Timusk and B. Statt, Reports on Progress in Physics 62, 61 (1999).

[2] D. S. Marshall, D. S. Dessau, A. G. Loeser, C-H. Park, A. Y. Matsuura, J. N. Eckstein, I. Bozovic, P. Fournier, A. Kapitulnik, W. E. Spicer, and Z.-X. Shen, Phys. Rev. Lett 76, 4841 (1996); M. R. Norman, H. Ding, M. Randeria, J. C. Campuzano, T. Yokoya, T. Takeuchi, T. Takahashi, T. Mochiku, K. Kadowaki, P. Guptasarma, D. G. Hinks, Nature 392, 157 (1998).

[3] K. M. Shen, F. Ronning, D. H. Lu, F. Baumberger, N. J. C. Ingle, W. S. Lee, W. Meevasana, Y. Kohsaka, M. Azuma, M. Takano, H. Takagi, and Z.-X. Shen, Science 307, 901-904 (2005).

[4] P. W. Anderson, Science 235, 1196 (1987).

[5] P. W. Anderson, P. A. Lee, M. Randeria, T. M. Rice, N. Trivedi, and F. C. Zhang, J. Phys.: Condense Matter, 24, R755 (2004).

[6] F. C. Zhang, C. Gros, T. M. Rice and H. Shiba, Supercond. Sci. Technol., 1, 36-46 (1988).

[7] Patrick A. Lee, Naoto Nagaosa, and Xiao-Gang Wen, Rev. Mod. Phys. 78, 17 (2006).

[8] C. Honerkamp, M. Salmhofer, N. Furukawa, and T. M. Rice, Phys. Rev. B 63, 035109 (2001); C. Honerkamp, M. Salmhofer, and T. M. Rice, Euro. Phys. J. B. 27, 127 (2002).

[9] R. M. Konik, T. M. Rice, A. M. Tsvelik, Phys. Rev. Lett 96, 086407 (2006).

[10] J. M. Luttinger and J. C. Ward, Phys. Rev. 118, 1417 (1960); J. M. Luttinger, Phys. Rev. 119, 1153 (1960).

[11] F. H. L. Essler, R. M. Konik in "*From Fields to Strings: Circumnavigating theoretical Physics*", ed. by M. Shifman, A. Vainshtein and J. Wheather, World Scientific, Singapore (2005); cond-mat/0412421.

[12] Matthias Troyer, Hirokazu Tsunetsugu and T.M. Rice, Phys. Rev. B 53, 251 (1996).

[13] Tai-Kai Ng, Phys. Rev. B 71, 172509 (2005).

[14] Xiao-Gang Wen and Patrick A. Lee, Phys. Rev. Lett. 76, 503 (1996); Xiao-Gang Wen and Patrick A. Lee, Phys. Rev. Lett. 80, 2193 (1998).

[15] J. W. Loram, K. A. Mirza, J. R. Cooper and J. L. Tallon, J. Phys. Chem Solids 59, 2091 (1998).

[16] A. A. Abrikosov, L. P. Gorkov and I. E. Dzyaloshinaskii, "*Methods of Quantum Field Theory in Statistical Physics",* ed. by R. A. Silverman, revised edn. Dover, New York; I. E. Dzyaloshinskii, Phys. Rev. B 68, 85113 (2003).

[17] A. M. Tsvelik, "*Quantum Field Theory in Condensed Matter Physics",* CUP, 2003.

[18] R. Konik and A. W. W. Ludwig, Phys. Rev. B64, 155112 (2001); R. Konik, F. Lesage, A. W. W. Ludwig and H. Saleur, Phys. Rev. B 61, R4983 (2000).

[19] M. C. Gutzwiller, Phys. Rev. Lett. 10, 159 (1963).

[20] A. Läeuchli, C. Honerkamp, and T. M. Rice, Phys. Rev. Lett. 92, 037006 (2004).

[21] M. R. Norman, M. Randeria, H. Ding and J. C. Campuzano, Phys. Rev. B 57, R11093 (1998).

[22] C. Honerkamp (private communication).

[23] L. F. Mattheiss, Phys. Rev. B 42, 354 (1990).

[24] Mohit Randeria, Arun Paramekanti, and Nandini Trivedi, cond-mat/0307217; Kai-Yu Yang, C. T. Shih, C. P. Chou, S. M. Huang, T. K. Lee, T. Xiang, F. C. Zhang, cond-mat/0603423.

[25] J. L. Tallon, J. W. Loram, G. V. M. Williams, J. R. Cooper, I. R. Fisher, J. D. Johnson, M. P. Staines, C. Bernhard, phys. stat. sol. (b) 215, 531 (cond-mat/9911157).

[26] M. R. Presland, J. L. Tallon, R. G. Buckley, R. S. Liu, and N. E. Flower, Physica C 176, 95 (1991).

[27] E. Fawcett, H. L. Alberts, V. Yu. Galkin, D. R. Noakes and J. V. Yakhmi, Rev. Mod. Phys. 66, 25 (1994).

[28] X. J. Zhou, T. Yoshida, A. Lanzara, P. V. Bogdanov, S. A. Kellar, K. M. Shen, W. L. Yang, F. Ronning, T. Sasagawa, T. Kakeshita, T. Noda, H. Eisaki, S. Uchida, C. T. Lin, F. Zhou, J. W. Xiong, W. X. Ti, Z. X. Zhao, A. Fujimori, Z. Hussain and Z.-X. Shen, Nature 423, 398 (2003).

[29] David Sénéchal and A.-M. S. Tremblay, Phys. Rev. Lett 92, 126401 (2004).

[30] Alexandru Macridin, Mark Jarrell, Thomas Maier, P. R. C. Kent, cond-mat/0509166.

[31] N. D. Mathur, F. M. Grosche, S. R. Julian, I. R. Walker, D. M. Freye, R. K. W. Haselwimmer, G. G. Lonzarich, Nature 394, 39 (1998).